# Vapor Phase Imaging of Diesel Fuel Sprays from a Common Rail Injector

P.V. Farrell and M.S. Beckman

Engine Research Center
University of Wisconsin-Madison
Madison, WI 53706 USA

An experiment for imaging the vapor region of an evaporating fuel spray was conducted in a constant volume spray chamber. The imaging method employed an exciplex fluorescence technique to quantify the vapor concentration of two-phase sprays. The injection system was a common rail design with multiple injection capability of a type typically found in heavy-duty applications. The major goals were to simulate the high temperature and pressure environment of a diesel engine, and examine the effect of multiple injections, particularly the characteristics of a short pilot vs. single injection event. The experimental conditions (ambient temperature, ambient pressure and injection pressure) were held constant. The experiment focused on the development of the spray up to the point where auto ignition would typically occur. A calibration procedure to account for laser characteristics, absorption, and temperature dependence, was applied to the images. The results from analyzing the images were temperature and equivalence ratio contour maps of the spray at various times after start of injection.

## 1. Introduction

Injection systems for direct injection engines with multiple injection capability have been shown to substantially reduce emissions of particulate with little change in $NO_X$ emissions [1,2,3]. This is an attractive option for engine designers to meet emission standards because it requires no additional hardware such as exhaust gas aftertreatment.

Tow *et al.* [1] conducted in-cylinder studies of the effect of multiple injections in a heavy-duty diesel engine, attempting injection strategies employing one, two and three injections per cycle for two different load conditions. Among the conclusions was that a relatively long dwell before the last injection appeared to be effective for particulate reduction. Also, the effect of split injection was an increase in fuel/air mixing and particulate oxidation rates late in the combustion period. The ability to effectively retard timing without increasing particulate was the main advantage of double and triple injection strategies for $NO_X$ reduction. From these conclusions, Tow *et al.* suggested an effective injection strategy for emission reduction: a small pilot injection (for $NO_X$ control), a long dwell (for particulate control) and a fast rise in the rate of the final injection. While subsequent studies [4] have indicated that different injection strategies (such as split injection) may be required to reach optimal emission reduction, the short pilot/long dwell injection strategy will be the focus of this paper.

This study seeks to examine the differences between the vapor region of spray plumes from a single injection and short pilot injection separated from the main injection by a long dwell. The focus will be on the early portion of injection, up to the point where auto ignition would normally occur. Since the ignition delay varies depending on operating conditions, [1] images were taken up to a point where ignition was certain to occur under

most conditions. The goal of the experiment was to determine whether the explanations for reduced particulate and $NO_X$ reported by Tow *et al.* [1] and studied numerically by Han *et al.* [5] were supported by the distribution of the vapor regions of the spray. To accomplish this, an experiment to image the vapor regions of an evaporating fuel spray in diesel-like conditions was conducted. The images were then evaluated as quantitative temperature and equivalence ratio contour maps using a calibration scheme.

The major results were that a short pilot injection caused a small region of rich fuel mixture to exist, while the single injection caused a larger region of richer fuel mixture to exist. In addition, there were lower peak equivalence ratios (lower temperature depressions) in the central 'core' of the pilot spray plumes. Finally, the short pilot injection showed much shorter spray penetration lengths with very little forward velocity.

## 2. Experimental Set-up

Images of the fuel sprays were taken inside a constant volume spray chamber with extensive optical access. To reproduce the in-cylinder conditions, a pre-charge combustion method was used. The chamber was filled with a slightly rich and highly diluted mixture of oxygen, acetylene, and nitrogen. This mixture was ignited and reached a temperature and pressure of approximately 2000 K and 8.6 MPa respectively, which corresponded to a density of 15 kg/m$^3$. The combustion products then cooled, and when the desired ambient temperature was reached, injection was initiated. The mixture (81% Nitrogen, 13% Air, and 6% Acetylene) was selected to minimise particulate formation, water condensation, and to leave no oxygen remaining after combustion, which would quench the fluorescence signal. This dictated that the sprays were non-combusting. The injection system was a Nippon-Denso common rail with the ability to produce up to three pilot injections. The specifics of the experiment, injector and nozzle are given in Table 1 below.

The fuel (dodecane) was doped with exciplex compound forming chemicals; naphthalene and TMPD (tetramethyl-p-phenylene diamine), and were mixed at 10 % and 1 % by mass respectively. These chemicals, when stimulated by a UV light source fluoresced with different spectra, depending on whether they were in the liquid or vapor phase [6]. A frequency tripled Nd:YAG laser at 355 nm was used to stimulate the dopant. The beam was formed into a sheet approximately 50 mm x 0.5 mm and sent through a side window of the chamber down the axis of one plume of the six plume injector. The fluorescence signal was collected normal to laser sheet through the main window of the chamber. Using a beamsplitter and appropriate filters, separate images of the liquid and vapor regions of the spray were acquired. Two separate images of the spray were taken using two intensified CID cameras. The experiment was controlled using LABVIEW, custom timing software, and two independent frame grabbers. Since the cameras were single shot, multiple realizations of the same experiment were required to resolve the temporal evolution of the spray.

**Table 1** Experimental conditions, and injector/nozzle specifics.

| Parameter | Value | Parameter | Value |
|---|---|---|---|
| Orifice Diameter | 260 μm | Nozzle Type | mini-sac |
| No. of Holes | 6 | Injection Pressure | 40 MPa |
| Orifice Length | 500 μm | Ambient Temperature | 1000 K |
| Spray Angle | 140 ° | Ambient Density | 15 kg/m$^3$ |

## 3. Calibration

Quantification of vapor images into equivalence ratio and temperature contour maps was accomplished using a technique outlined by Kim and Ghandhi [7] and Kim *et al.* [8]. The conversion of images was done via software, which compensates for temperature dependant TMPD fluorescence, absorption through the spray, and laser sheet profile. The pixel intensity measured at the camera, $S_{LIF}$, can be related to the TMPD concentration, $N_{TMPD}$, by the following equation (1).

$$S_{LIF} = K \cdot N_{TMPD} \cdot \frac{I_i}{I_o} \cdot f(T) \tag{1}$$

The function *f(T)*, temperature dependence of TMPD, was determined previously [7] while the ratio of actual to incident intensities was given by the Lambert-Beer absorption law (2):

$$\frac{I_i}{I_o} \equiv \exp\left( -\int_0^L \sigma_{TMPD} \cdot N_{TMPD} \cdot dl \right) \tag{2}$$

where $L$ was the length of the spray over which absorption occurs, and $\sigma_{TMPD}$ was the absorption coefficient for TMPD. The temperature was determined using a conservation of energy assumption. The assumption was that the energy required to heat the liquid fuel, vaporize the fuel, and then heat the vapor comes from the adjacent ambient gas [9,10]. From this assumption, the equation to determine temperature is given below (3).

$$\int_{T_{mix}}^{T_{amb}} C_{p,a} dT = \chi_{F/A} \left[ \int_{T_{f,i}}^{T_{\text{int}}} C_{p,liquid} dT + h_{v,T_{\text{int}}} + \int_{T_{\text{int}}}^{T_{mix}} C_{p,vapor} dT \right] \tag{3}$$

Finally, to close the system of equations the system constant $K$ was determined by integrating all pixels and comparing the calculated total fuel mass with the known fuel mass. This calculation is given in equation 4 below:

$$m_{total} = \int_0^{2\pi} \int_0^R \int_0^L N_{TMPD} \cdot r \cdot dl \cdot dr \cdot d\phi \tag{4}$$

where $N_{TMPD}$ was integrated over the entire length and radius of the spray. The preceding equations (1-4) were solved to determine the system constant, $K$.

To solve the equation set (1-4) an image with a known amount of fuel vapor present was required. This was accomplished by taking 'calibration' images of short injection events (~500μs injection duration). Images of these injection events approximately 700 μs after start of injection were assumed to contain only fuel vapor. From injection bench tests at the same injection pressure the mass of fuel vapor was determined, $m_{total}$. Using the known $m_{total}$ with equations 1-4 the system constant, $K$, can be calculated iteratively.

Once the system constant was determined, the equations (1-3) were solved iteratively for each pixel of each image. The results were temperature and equivalence ratio contour maps of the spray.

## 4. Results

Two series of images of evaporating fuel sprays calibrated into equivalence ratio and temperature contour maps are given in Figures 1 and 2.

Figure 1 shows the spray from a single injection 2000 μs in width. Images were taken from 345-825 μs ASI (After Start of Injection). Each image was from a different injection event and shows substantial shot-to-shot variation in the spray shape and equivalence ratios/temperatures. Apparent in the images were steep transitions in equivalence ratio from the central 'core' region to the sides and head of the spray. This was consistent with other research [11,12,13] that had shown very steep gradients along the lateral edges of the spray. The peak equivalence ratios in the center of the plumes in Figure 1 were between 1.5 and 2.0 depending on the time ASI. The values from Figure 1 agree with some other research; however, results cited in the literature can vary widely [9,11,12,13,14,15]. The differences among these results can be attributed to the various ambient conditions and injection pressures under which the measurements were taken. Flynn *et al.*, for example, [14] reported higher peak equivalence ratios of $\phi$ = 2-4 for sprays at ~1000 K and 16.6 kg/m$^3$ (similar to the conditions for this study) using results from a Rayleigh scattering measurement technique.

Figure 2 shows the spray from a 400 μs pilot injection with a 996 μs dwell. Images were taken from 800-1350 μs ASI. The images do not show the main injection event (which starts at approximately 1396 μs ASI) since ignition would have already occurred under these conditions. Since this was a non-combusting spray, images after the point of auto ignition were not considered since the heat release from combustion would influence the vaporization. The pilot injection had a much lower equivalence ratio within the 'core', (the peak equivalence ratios were 1.0 to 1.5) than the single injection case. The images also showed that the gradients along the sides and head of the spray were much less steep than the single injection case. Since all the images in Figure 2 were after the pilot injection had ended, it was expected that the spray would be better mixed (less steep gradients) than the single injection case because the 'core' was no longer being supplied with liquid fuel.

Another difference between the single and pilot injection were the vapor penetration length and velocity. Figure 3 shows the vapor penetration length measured at the $\phi$ = 1.0 and $\phi$ = 0.2 contours for both the single and pilot plumes. The penetration lengths for the single injection were longer than for the pilot injection. This was caused by the pilot injection not reaching peak injection pressures since the duration was too short. This can be seen in the injection rate curves for both cases, Figure 4. Since increased injection pressure increases vapor penetration length [16], the lower injection pressure of the pilot injection resulted in shorter penetration lengths. The single injection also had increasing penetration length over the entire measured time duration, while the penetration length of the pilot injection was relatively constant over the measured time duration. This indicates that the vapor velocity of the pilot injection had gone to zero. The short pilot injection had ended before the first available image (~795 μs ASI). This meant that the momentum source, incoming liquid fuel, had already ended before the first image was acquired. Zero penetration velocity indicates that most of the initial injection momentum had been dissipated and that diffusion and ambient gas flow were the only drivers for fuel mixing.

From Figures 1 and 2 the maximum temperature depressions in the central 'core' region were found to be ~175 K for the single injection case and ~125 K for the pilot injection case. Both of these results estimate a larger temperature depression when compared to other research [9,14]. These differences were likely the result of the differences in the

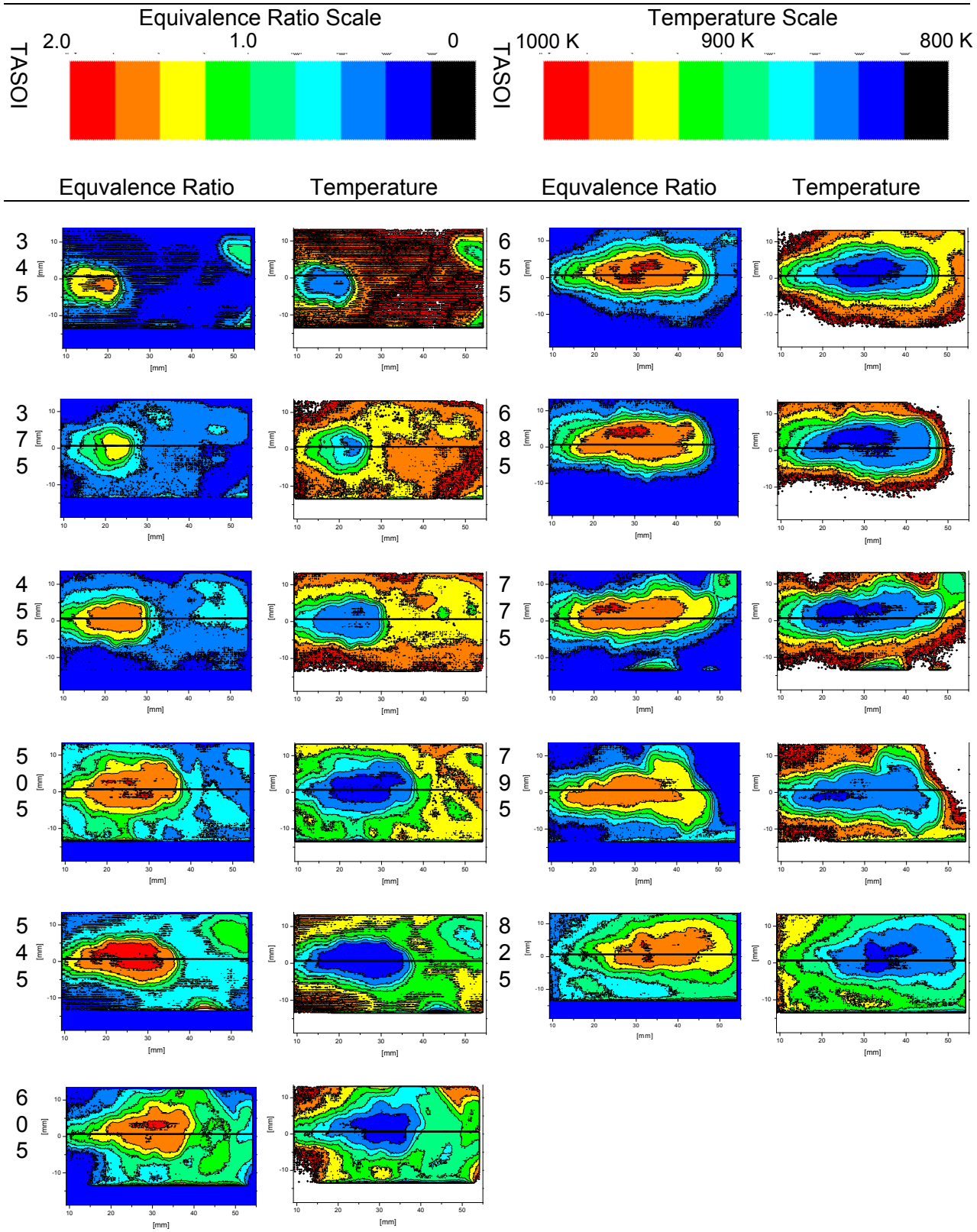


**Figure 1** Equivalence ratio and temperature contour maps of single injection spray. (40 MPa injection pressure, 1000 K ambient temperature and single injection 2000μs) TASOI-Time After Start Of Injection [μs]

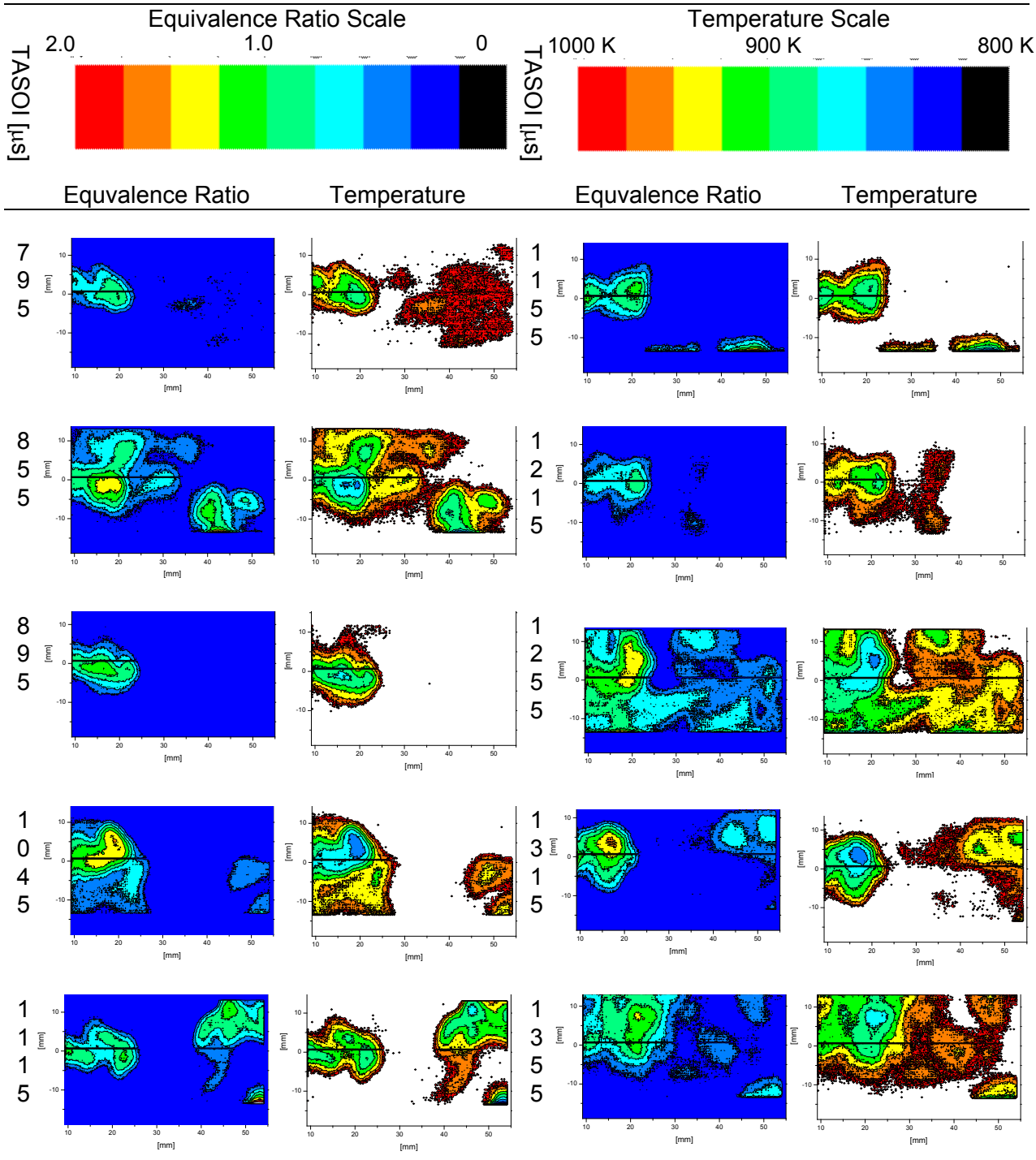


**Figure 2** Equivalence ratio and temperature contour maps of pilot injection spray. (40 MPa injection pressure, 1000 K ambient temperature and pilot injection 400 μs with 996 μs dwell. TASOI-Time After Start Of Injection [μs]

assumptions used to determine the temperature for calibration [14], or that the temperature depression was more sensitive to equivalence ratio as ambient temperature increased [9].

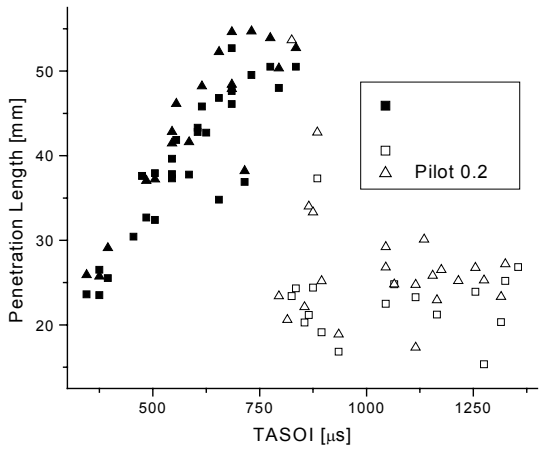


**Figure 3** Penetration lengths of single and pilot injection measured at $\phi = 1.0$ and $\phi = 0.2$ contours.

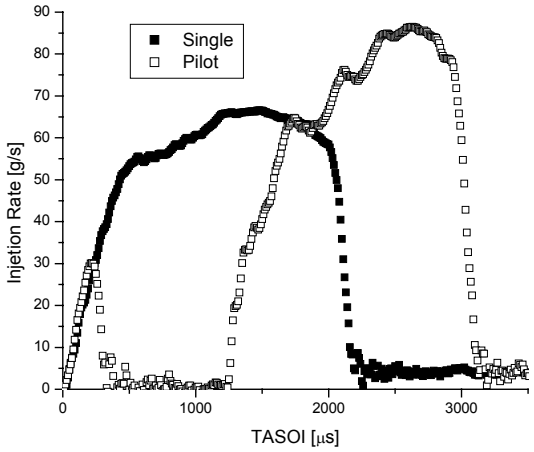


**Figure 4** Injection rate from single and pilot injection experiments.

## 5. Conclusions

Based on comparisons of the contour maps from the pilot and single spray plumes the following conclusions are presented for the conditions given in Table 1:

- Pilot injections showed overall lower equivalence ratios compared to single injections, with smaller rich mixture extent.
- Pilot injections showed lower temperature depression compared to single injections, a result of the lower equivalence ratios and temperature assumption.
- Pilot injections showed less steep temperature and equivalence ratio gradients at the spray periphery compared to single injections.
- Pilot injections showed overall shorter penetration lengths compared to single injections.

## 6. Nomenclature

| | |
|---|---|
| $c_p$ | specific heat |
| $f(T)$ | temperature dependence of TMPD |
| $h_v$ | heat of vaporisation |
| $I$ | intensity of laser sheet |
| $K$ | system constant |
| $L$ | absorption length/spray length |
| $m_{total}$ | mass in spray |
| $N_{TMPD}$ | TMPD concentration at pixel |
| $S_{LIF}$ | pixel intensity |
| $T$ | temperature |
| $X_{F/A}$ | mass percentage fuel/air |
| $\sigma_{TMPD}$ | absorption coefficient of TMPD |

*Subscripts*

| | |
|---|---|
| *o* | incident intensity |
| *i* | intensity at pixel |
| *liquid* | liquid |
| *vapor* | vapor |
| *a* | ambient gas |
| *amb* | ambient |
| *mix* | mixture |
| *int* | boiling point |
| *f,i* | initial fuel |

## 7. References


[1] Tow, T. C., Pierpont, D. A. and Reitz, R. D.; "Reducing Particulate and $NO_X$ Emissions by Using Multiple Injections in a Heavy Duty D.I. Diesel Engine"; SAE Paper 940897; 1994.

[2] Pierpont, D. A., Montgomery, D. T. and Reitz, R. D.; "Reducing Particulate and $NO_X$ Using Multiple Injections and EGR in a D.I. Diesel"; SAE Paper 950217; 1995.

[3] Montgomery, D. T. and Reitz, R. D.; "Six-Mode Cycle Evaluation of the Effect of EGR and Multiple Injections on Particulate and $NO_X$ Emissions from a D.I. Diesel Engine"; SAE Paper 960316; 1996.

[4] Montgomery, D T.; "An Investigation into Optimization of Heavy-Duty Diesel Engine Operating Parameters when Using Multiple Injections and EGR"; Ph.D. Thesis; University of Wisconsin-Madison; 2000.

[5] Han, Z., Uludogan, A., Hampson, G.J. and Reitz, R.D.; "Mechanism of Particulate and $NO_X$ Emission Reduction Using Multiple-Injection in a Diesel Engine"; SAE Paper 960633; 1996.

[6] Melton, L. and Verdieck, J.; "Vapor/Liquid Visualization for Fuel Sprays"; Combustion Science and Technology; Vol. 42, pp 217-222; 1985.

[7] Kim, T. and Ghandhi, J.B.; "Quantitative 2-D Vapor Concentration Measurements in an Evaporating Diesel Spray using the Exicplex Fluorescence Method"; SAE Paper 2001-01-3495; 2001.

[8] Kim, T., Beckman, M.S., Farrell, P.V. and Ghandhi J.B.; "Evaporating Spray Concentration Measurements from Small and Medium Bore Diesel Injectors"; SAE Paper 2002-01-0219; 2002.

[9] Yeh, C., Kamimoto, T., Kosaka, H. and Kobori, S.; "Quantitative Measurement of 2-D Fuel Vapor Concentration in a Transient Spray via Laser-Induced Fluorescence Technique"; SAE paper 941953; 1994.

[10] Senda, J. and Kanda, T.; "Quantitative Analysis of Fuel Vapor Concentration in Diesel Spray by Exciplex Fluorescence Method"; SAE Paper 970796; 1997.

[11] Suzuki, M., Nishida, K. and Hiroyasu, H.; "Simultaneous Concentration Measurement of Vapor and Liquid in an Evaporating Diesel Spray"; SAE Paper 930863; 1993.

[12] Bruneaux, G.; "Quantitative Visualisation of Vapor Phase in a High Pressure Common Rail Diesel Injection"; *Eighth International Conference on Liquid Atomisation and Spray Systems*; Pasadena, CA, USA; 2000.

[13] Bruneaux, G., Verhoeven, D. and Baritaud, T.; "High Pressure Diesel Spray Combustion Visualization in a Transport Model Diesel Engine"; SAE Paper 1999-01-3648; 1999.

[14] Flynn P., Durrett, R., Hunter, G., zur Loye A., Akinyemi, O., Dec J. and Westbrook C.; "Diesel Combustion: An Integrated View Combining Laser Diagnostics, Chemical Kinetics, And Experimental Validation"; SAE Paper 1999-01-0509; 1999.

[15] Minami, T., Yamaguchi, I., Shintani, M., Tsujimura, K. and Suzuki, T.; "Analysis of Fuel Spray Characteristics and Combustion Phenomena under High Injection Pressure Fuel injection"; SAE paper 900438; 1990.

[16] Verhoeven, D., Vanhemelryck, J. -L. and Baritaud, T.; "Macroscopic and Ignition Characteristics of High-Pressure Sprays of Single-Component Fuels"; SAE Paper 981069; 1998.